A new look at density limits in tokamaks

A NEW LOOK AT DENSITY LIMITS IN TOKAMAKS

M. GREENWALD, J.L. TERRY, S.M. WOLFE
Plasma Fusion Center,
Massachusetts Institute of Technology,
Cambridge, Massachusetts

S. EJIMA*
General Atomic Technologies,
San Diego, California

M.G. BELL, S.M. KAYE
Princeton Plasma Physics Laboratory,
Princeton University,
Princeton, New Jersey

G.H. NEILSON
Oak Ridge National Laboratory,
Oak Ridge, Tennessee

United States of America

ABSTRACT. While the results of early work on the density limit in tokamaks from the ORMAK and DITE groups have been useful over the years, results from recent experiments and the requirements for extrapolation to future experiments have prompted a new look at this subject. There are many physical processes which limit the attainable densities in tokamak plasmas. These processes include: (1) radiation from low Z impurities, convection, charge exchange and other losses at the plasma edge; (2) radiation from low or high Z impurities in the plasma core; (3) deterioration of particle confinement in the plasma core; and (4) inadequate fuelling, often exacerbated by strong pumping by walls, limiters or divertors. Depending upon the circumstances, any of these processes may dominate and determine a density limit. In general, these mechanisms do not show the same dependence on plasma parameters. The multiplicity of processes leading to density limits with a variety of scaling has led to some confusion when comparing density limits for different machines. The authors attempt to sort out the various limits and to extend the scaling law for one of them to include the important effects of plasma shaping, i.e. $\bar{n}_e = \kappa \bar{J}$, where n_e is the line average electron density (10^{20} m^{-3}), κ is the plasma elongation and $\bar{J}$ (MA·m^{-2}) is the average plasma current density, defined as the total current divided by the plasma cross-sectional area. In a sense, this is the most important density limit since, together with the q-limit, it yields the maximum operating density for a tokamak plasma. It is shown that this limit may be caused by a dramatic deterioration in core particle confinement occurring as the density limit boundary is approached. This mechanism can help explain the disruptions and Marfes that are associated with the density limit.

1. INTRODUCTION

In exploring the operating regime of a tokamak, researchers have always found a limit in the maximum density that they could achieve. Attempts to raise the density beyond this limit result in a disruption of the discharge. The value of the density limit is found to vary from machine to machine and with operating conditions in a systematic way. In this paper, we consider several distinct limits. The first is the familiar Murakami limit, with $n_e < B_T/R$ [1]. The coefficient m is not constant but increases with input power and with plasma purity. A second and distinct limit is apparent when density is plotted against plasma current or (when these are normalized to the toroidal field) as Murakami number, $n_e R/B$ versus $1/q$ [2, 3]. This is the DITE (or Hugill) plot and in this paper we use the term 'Hugill limit' to refer to density limits with $n_e \sim I_p$ [4]. Of course, experimental and theoretical investigations of these limits do not always yield such clear and simple scalings. In a

* Present address: Shin-Etsu Chemical Co., Ltd, 2-13-1, Isobe Annaka, Gunma, Japan.

later section, we suggest that it might be more appropriate to distinguish between the limits by their underlying mechanism, i.e. we would use 'Murakami limit' to refer to operational limits imposed by plasma radiation and 'Hugill limit' to refer to limits imposed by deterioration of particle confinement. For completeness, we include a third limit, associated with an MHD threshold phenomenon that was observed by Granetz on Alcator C [5]. This behaviour is not well understood, but it leads to a density limit with $n_e \sim B^2$. Finally, there is a density limit which is imposed by the fuelling process itself. Gas puffing alone is not always sufficient to reach the Murakami or Hugill limits. It is important to understand that all the density limits must be obeyed; the operating space of a tokamak is limited by the minimum of the Murakami, Hugill, Granetz and fuelling limits.

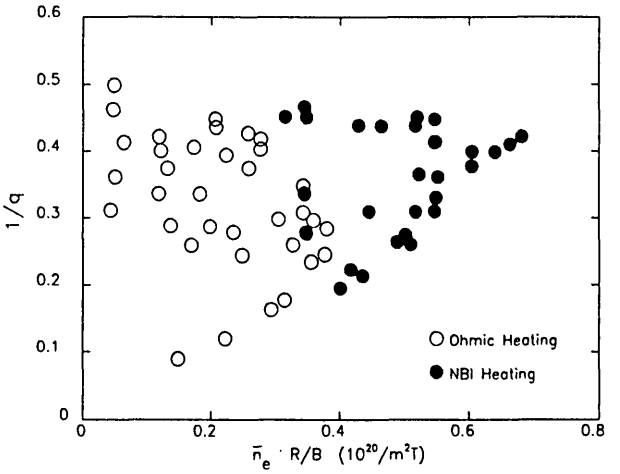

FIG. 1. DITE (or Hugill) plot for DITE plasmas. Each point represents an individual discharge and the operating range is given by the envelope of these points.

2. SCALING AND DEPENDENCES OF THE DENSITY LIMITS

2.1. Murakami limit

The Murakami limit was first proposed as an empirical scaling for the highest density achievable under any given discharge conditions. The B/R scaling brought together results from a very wide range of machines working at density limits that varied over two orders of magnitude. The scaling was never exact, of course, and as experimenters refined their techniques, particularly in the control of impurities, densities well above the original limit were subsequently reached. This gave rise to the use of the Murakami number, which is simply the line average density divided by B_T/R. This allowed density limits to be compared under different conditions, while normalizing out the strongest dependence. The Murakami number was seen to increase as Z_{eff} approached one [6] and as additional heating, in the form of neutral beams, was applied [3, 7]. This density limit has been attributed to a loss of balance between input power and radiated power [1, 8].

2.2. Hugill limit

Additional insight into tokamak operational limits was obtained when plasma density was plotted against plasma current (or, in their normalized form, as Murakami number versus 1/q) for a large number of discharges [4]. The earliest plots of this kind are from DITE, for which data are shown in Fig. 1 [9]. The operational limits are determined from the boundaries of data in these plots. Three important features can be seen in this figure [10, 11]. First, there is a density limit proportional to the plasma current; second, the proportionality constant between maximum density and plasma current is not increased with auxiliary heating; third, auxiliary heating allows the maximum density to be achieved at higher plasma currents. We can understand the data in Fig. 1 as resulting from the superposition of the limit on q ($q > 2$) and two distinct density limits: a 'Hugill' limit with $n_{max} \propto I_p$ independent of input power, and a Murakami limit with n_{max} independent of I_p but strongly influenced by input power.

The operating space for all tokamaks shows the same general features. This is presented in schematic form in Fig. 2, in which the various limits identified by us are indicated. The use of the standard normalized axes, I_p and the Murakami number permits a direct comparison among machines. Figure 3 shows the DITE plot with data for several different tokamaks. For clarity, only the boundaries of experimentally accessible regions are drawn instead of including data points from individual discharges. If all machines showed the same Hugill density limit, $n_{max} = B/qR$, the lower boundary of each region should coincide. Although, to lowest order, the chosen normalization does bring together data from devices with widely varying parameters, it is clear from this figure that substantial systematic differences between the devices remain. In particular, we note that machines capable of producing strongly

shaped plasmas reach the highest values of n_e/I_p. Of course, differences between the density limits on various machines may be due to differences in experimental technique, or to differences, from machine to machine, in the physics that sets the density limit. Neither of these alternatives is very attractive since they do not help us understand the physics of the limits nor do they allow us to extrapolate to density limits on future machines. Fortunately, if past experience is a guide, we can say that we simply do not have quite the right scaling expression.

Under the assumption that there is a common cause for this density limit on all machines, we can look for a scaling that brings all the data into line. We can begin by noting that the equation $n_{max} \sim B/qR$ is close (within a factor of two) to the expression we are seeking and thus we can use, as a first approximation, $n \sim I_p/a^2$. It should be pointed out that there is no consensus in the literature on which 'form' of q to use in plotting the density limit. Various approximations of q_ψ and $q_{cylindrical}$ are used, together with expressions such as $q = 5a^2B/IR$, which are only correct for circular machines and in the limit of high aspect ratio and low beta. If the plasma safety factor is important in the physics of the density limit rather than being simply a convenient normalization of the plasma current, then we would expect q_ψ to be the correct term to use. Data from Alcator C, D-III and PBX are plotted against q_ψ in Fig. 3. This is not the scalling we are looking for; q_ψ does not seem to be an important quantity with respect to the density limit.

By fitting the available data to very simple combinations of the machine parameters, we arrive at an expression that does bring together data from the various machines, namely

$$\bar{n} = \kappa \bar{J} \qquad (1)$$

measured in 10^{20} m^{-3}, where κ is the plasma elongation and $\bar{J}$ is the average plasma current density, with the I_p area measured in $MA \cdot m^{-2}$. Figures 4a to 4d are modified Hugill plots for several machines, showing the results of this scaling. They should be compared with Fig. 3. For elliptical machines this scaling for the density limit can be written as $\bar{n}_{max} = I_p/\pi a^2$, and for high aspect ratio, low beta, circular machines it can be written as $(5/\pi) \times B/qR$. A few comments on the simplicity of Eq. (1) are in order. It is almost certain that the dependences on plasma size and elongation given by Eq. (1) are not exact and that additional dependences on shape parameters exist. By its nature, the density limit boundary can only be approximately defined. As the limit is approached, the plasma becomes increasingly susceptible to disruption and data become sparser so that, aside from ordinary errors in the measurement of experimental quantities, the definition of the boundary is somewhat subjective. Data that would permit a more precise calculation of the parametric dependences are not easily obtained.

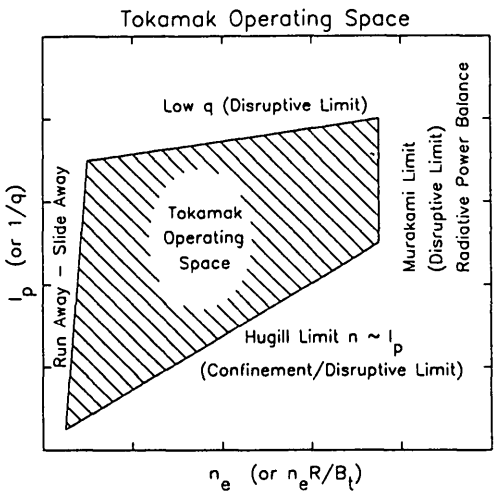

FIG. 2. Schematic for the DITE plot, with operating limits identified.

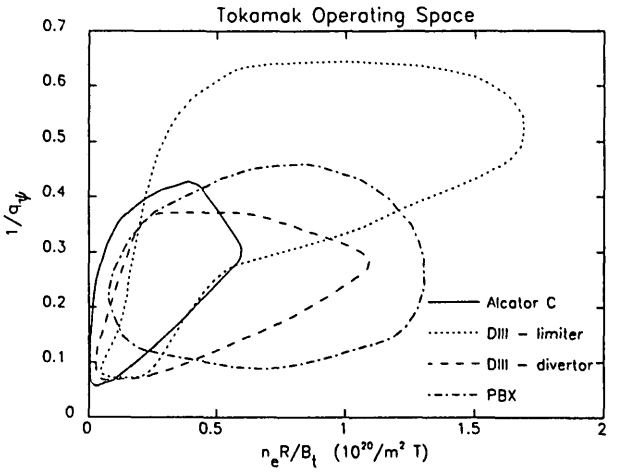

FIG. 3. DITE plot comparing data from Alcator C, D III and PBX. The abscissa is explicitly $1/q\psi$.

2.3. Fuelling related limits

The importance of an adequate fuel source in reaching a density limit seems obvious but is often overlooked (consider the density 'limits' that were observed before the technique of gas puffing was

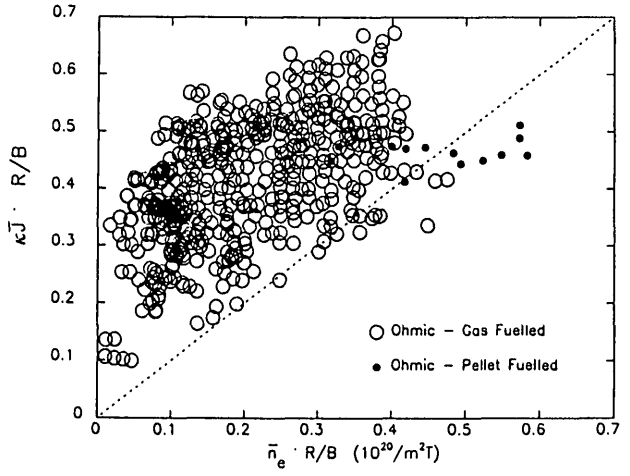

FIG. 4a. Alcator C density limits.
Plot of density versus the scaling parameter κJ for the same data as in Fig. 3.

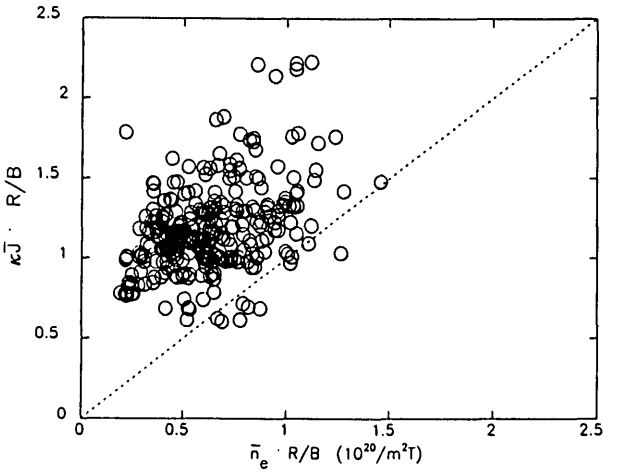

FIG. 4d. PBX density limits.
Plot of density versus the scaling parameter κJ for the same data as in Fig. 3.

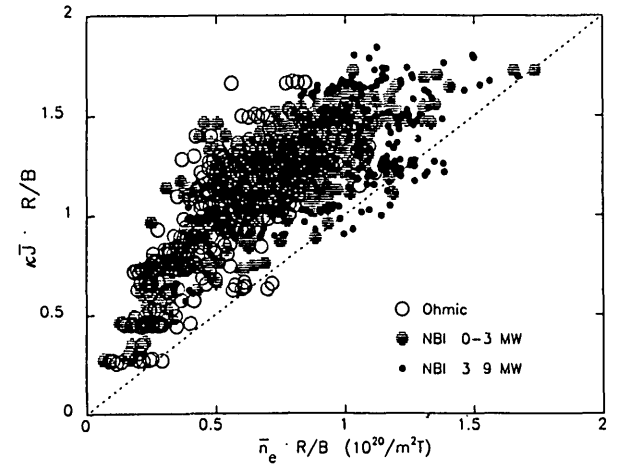

FIG. 4b. D III (limiter) density limits.
Plot of density versus the scaling parameter κJ for the same data as in Fig. 3.

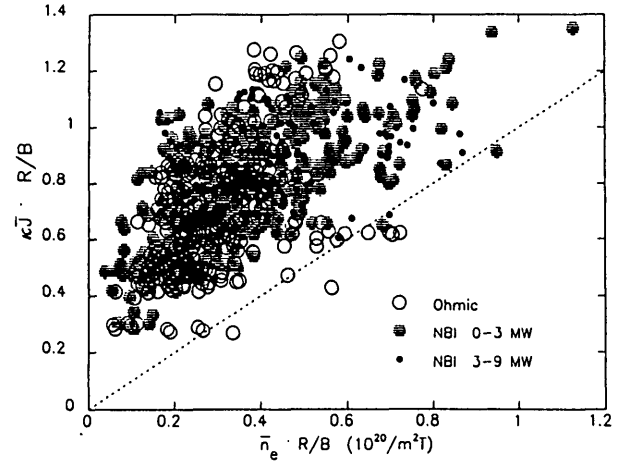

FIG. 4c. D III (divertor) density limits.
Plot of density versus the scaling parameter κJ for the same data as in Fig. 3.

introduced). As machines have become larger and denser, the mean free path for low energy neutrals has become smaller in comparison with the minor radius, and gas fuelling has become less effective. This can be clearly seen in DITE plots for JET and TFTR where Ohmic, gas fuelled plasmas are compared with plasmas fuelled by pellet injection (Fig. 5) [12, 13]. Injection of high speed, frozen hydrogen pellets introduces fuel directly into the plasma core, avoiding the limitations associated with gas puffing. The same effect can be achieved by fuelling with neutral beams (Fig. 6 [13]), which can yield the same plasma densities as pellet fuelling and Ohmic heating. In this case, the high densities have been attributed to the additional power that is added together with the particles [13]. However, in JET discharges with RF heating, without addition of particles, the same low densities as in gas fuelled Ohmic plasmas have been obtained. This has been explained as being due to additional impurities introduced by RF heating. If this were the case, plasmas with RF heating and NBI would not reach the same densities as plasmas with NBI alone, since impurities would be added by RF in both cases. This is contradicted by experimental data, which show that RF + NBI plasmas achieve the same densities as NBI or pellet fuelled discharges. Another clear example of a fuelling related density limit is given by the data from Alcator C (Fig. 7). The highest densities obtainable for machines configured with carbon limiters and gas fuelling are about half of those obtained in machines with molybdenum limiters. That this difference is due to deficient fuelling can be seen by observing that pellet fuelled plasmas with carbon limiters have the same density limit as those with molybdenum limiters.

Presumably, the strong pumping effect of carbon accounts for the difference seen with gas fuelling [14]. A similar effect probably accounts for the higher densities reported on TFTR with helium gas compared to hydrogen or deuterium [15, 16]. Limiters, walls and divertors can all compete effectively with the plasma for hydrogen fuel at the plasma edge.

2.4. Granetz limit

For completeness, we identify an additional density limit associated with an MHD threshold phenomenon. On Alcator C, low-m coherent MHD oscillations were observed when the line average density n_e was raised above $\sim B^2$ [5] (Fig. 8). This limit did not scale with plasma current over a wide range ($2.7 < q < 4.7$). The MHD amplitude increased rapidly for $n > n_c$ until, at densities about 40% above the MHD threshold, a disruptive density limit was reached. This behaviour was not seen on other machines. The results of a later study, showing a significant size scaling with $n_c \approx a^2$ or more [12], may provide an explanation for this. It is interesting to note that a strong degradation in impurity confinement was correlated with a rise in MHD activity, $1/\tau_I \sim (n-n_c)^4$ [18].

3. PHYSICS OF THE DENSITY LIMITS

The operating space for a tokamak is bounded in most cases by the occurrence of major disruptions. It would be wrong, of course, to look for the cause of the operational limits solely in the MHD equations (where electron density does not enter explicitly). It may be useful to think of the destruction of the MHD equilibrium as the final (fatal) symptom of some other underlying malady. For some time [1, 8], excessive radiation was assumed as the cause behind the density limit disruption. This is logical, since radiated power increases with density but input power does not. As radiation losses increase, the plasma temperature profile and the plasma current channel both shrink, which leads ultimately to the loss of MHD stability. Several authors derived expressions for a density limit determined by this mechanism that are in rough agreement with experimental measurements.

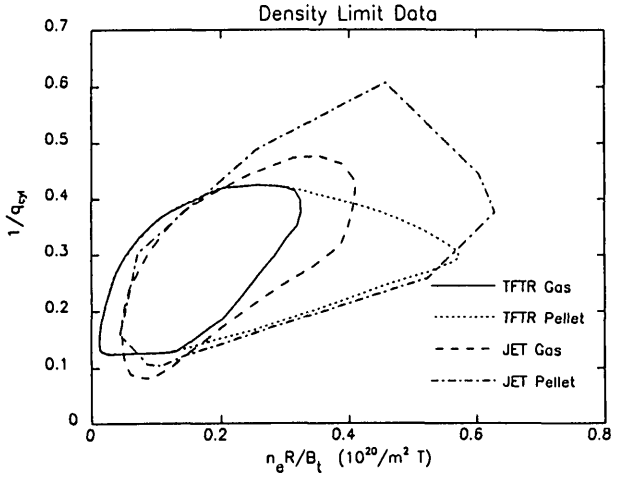

FIG. 5. Comparison of the operating space for gas and pellet fuelled discharges for the two large tokamaks JET and TFTR. The limits established with gas fuelling are easily overcome with an adequate fuelling technique.

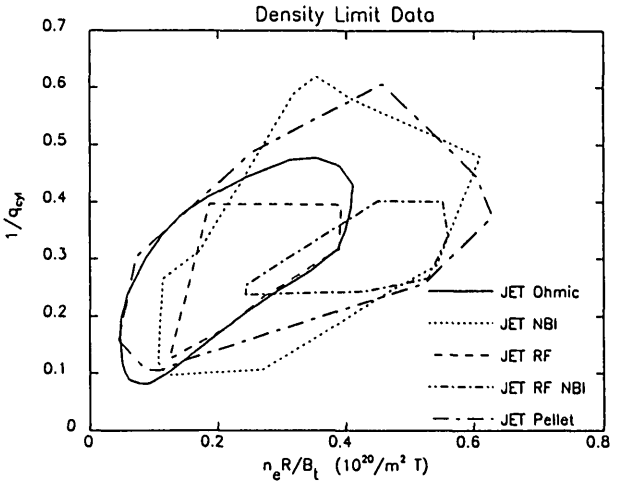

FIG. 6. Comparison of the operating space for JET discharges with Ohmic, NBI, ICRF and NBI + ICRF heating.

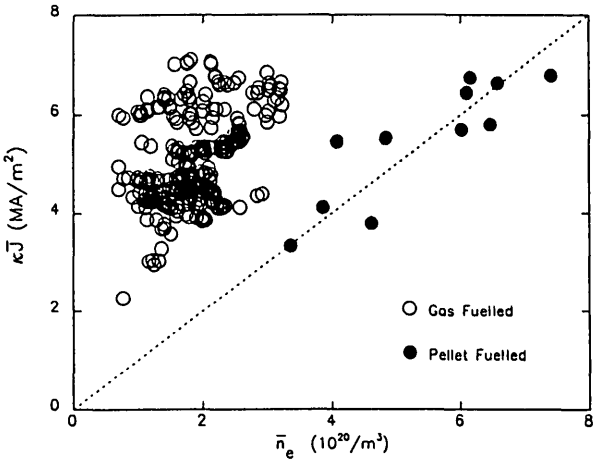

FIG. 7. Alcator C data taken with carbon limiters. The solid points are for discharges with pellet fuelling and carbon limiters. The dashed curve is for gas fuelled plasmas and molybdenum limiters.

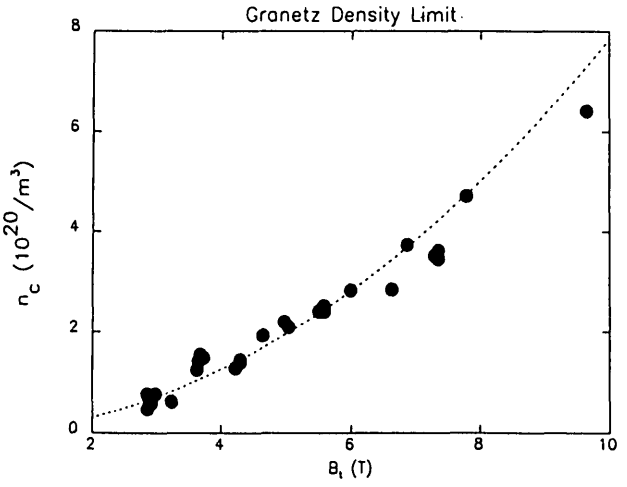

FIG. 8. The Granetz threshold for MHD activity (Alcator C). A density limit is found about 40% above the MHD threshold.

Gibson [19], Ohyabu [20], Ashby and Hughes [21], Wesson et al. [22] and Roberts [23] calculated the conditions required for thermal instability and MHD collapse due to impurities radiating in thin shells at the plasma boundary. Ashby and Hughes [21] found, for example, the following expression:

$$n_{max} \sim \frac{B}{qR}\left(\frac{Z_{eff}}{Z_{eff}-1}\right)^{1/2}\frac{1}{\bar{T}_e^{1/2}} \qquad (2)$$

Perkins and Hulse [24] calculated a density limit by requiring power balance between input power and radiated power in the plasma core. The expressions they derive can be written as

$$n_{max} \sim \frac{1}{(Z_{eff}-1)^{1/2}}\frac{B}{R} \qquad (3)$$

which agrees with Murakami's scaling and mechanism. Observations appear to support these models; the highest densities are achieved with auxiliary heating and in clean discharges (low Z_{eff}).

Closer inspection of the data reveals some problems with this picture. While the higher densities are reached at higher input power, the slope of n_{max} versus I_p is not much affected (Figs 1, 4), at least for plasmas with adequate fuelling (see Section 2.3). This was recognized by Hugill et al. [10,11], who suggested that radiation may not be responsible for this density limit. For relatively clean plasmas, this boundary is not dependent on impurity level either. In Fig. 9, the ratio of the measured density to the density limit, $\bar{n} = \kappa\bar{J}$, is plotted against Z_{eff}. It can be seen that the density limit is accessible for Z_{eff} up to 1.5 and perhaps as high as $Z_{eff} = 2$. Data from ISX-B (Fig. 10) show a similar result for a comparison of discharges from gettered and ungettered vacuum chambers. In contrast, the theoretical treatments diverge as $Z_{eff} \to 1$, limited only by hydrogen bremsstrahlung, which is overwhelmed by impurity radiation in the outer regions of the plasma at Z_{eff} only slightly above 1.

Results from a series of pellet fuelling experiments on Alcator C [25] suggest an alternative approach to this problem. In these experiments, single pellets were injected into plasmas with relatively low plasma current. The density increased very quickly at the time of injection (0.27 s) for all discharges and the rate of density decay was monitored (Fig. 11). As the plasma current was lowered from shot to shot, the decay time decreased dramatically. The calculations summarized in Table I show that the density limit, established with gas fuelling, was greatly exceeded. These discharges did not disrupt, however, but simply 'shed' particles in excess of the limit. The density decay time is not the same as the particle confinement time but is closely related. At steady state, the particle confinement is given by the ratio of density to source; however, in those cases where the time derivative dominates the source term, the density decay time will equal the particle confinement time τ_p. Unlike the conventionally defined global τ_p, which is dominated by the large particle fluxes in the plasmas edge, this confinement time is characteristic of the plasma core. It is worth pointing out that no decline in energy confine-

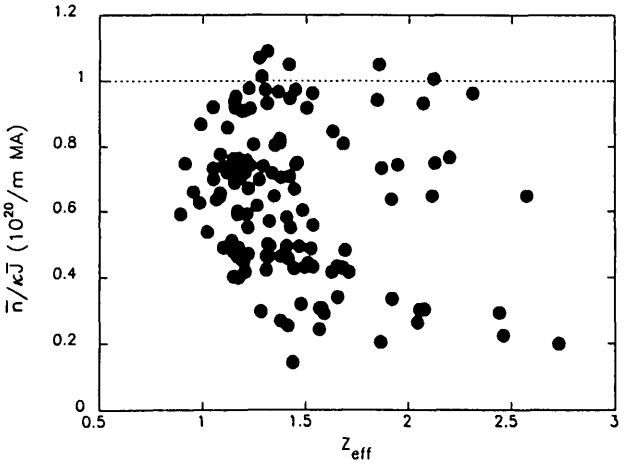

FIG. 9. Density (normalized to κJ) versus Z_{eff}. The dashed curve, which represents the scaled limit, $\bar{n} = \kappa\bar{J}$, can be reached for plasmas with Z_{eff} substantially above 1 (Alcator C).

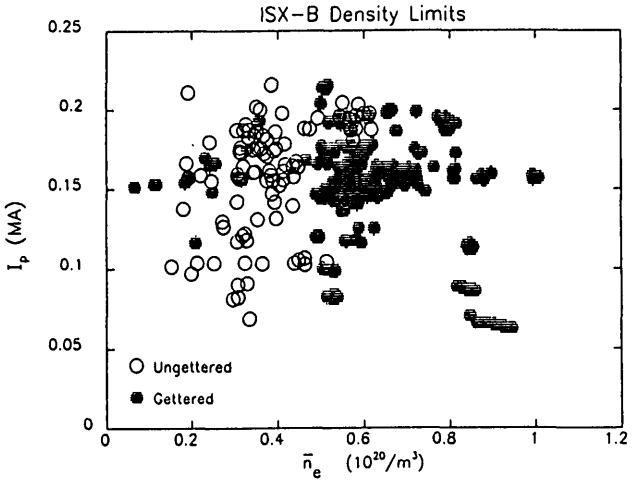

FIG. 10. ISX-B data comparing gettered and non-gettered discharges. While the highest densities are reached in gettered plasmas, the $n \sim I_p$ limit is essentially unaffected.

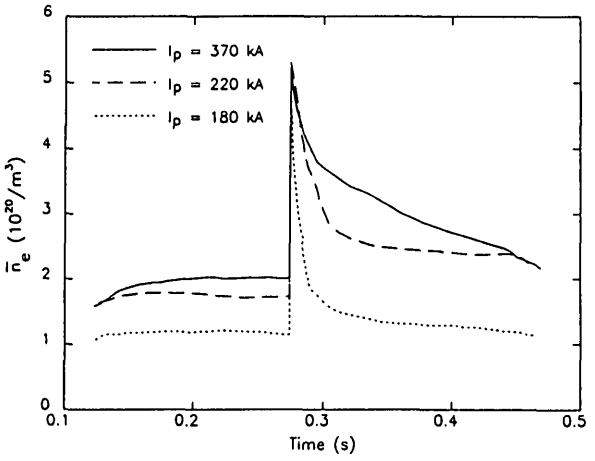

FIG. 11. Density decay after injection of a single pellet for discharges with different plasma currents (Alcator C).

ment accompanied the drop in particle confinement except for the convective loss directly associated with the density decay.

Figure 12 shows the results when the density decay time is plotted versus $\bar{J}/\bar{n}$ for a large collection of shots. The precipitous drop in particle confinement occurs in the neighbourhood of the previously derived density limit. The same data are plotted in another form in Fig. 13, which is a conventional DITE plot where data from pellet shots with fast decay rates are also shown. Table I presents data from Fig. 11. Shown for each shot are the plasma current I_p, the ratio of the maximum density for each discharge to the density limit $\kappa\bar{J}$, the calculated density limit n_{limit} and the density decay time τ_n from a fit to the curve (which is necessarily taken after the peak of the density).

If the deterioration of particle confinement described above is a general feature of tokamak discharges, it could be the prime force behind the density limit. (At the least, it allows us to push the chain of cause and effect back one more step. We need to add here that while this may explain various aspects of the density limit, the authors offer no insight into the physical mechanism that might lie behind the transport deterioration.) This does not mean that radiation does not play an important role in the $n \sim I_p$ limit. With deteriorating confinement, an ever larger source of fuel is needed for each incremental increase in density as a machine is pushed towards the limit. This will result in higher edge densities, more radiation and lower edge temperatures. Ultimately, the current profile and MHD stability are sufficiently altered to cause a major disruption. Of course, even in the absence of radiation, convective, ionization and charge exchange losses would eventually lead to the same result. (Allen et al. [26] reported that increased energy transport in the plasma periphery plays a role in density limit disruptions in the DITE tokamak.) With pellet fuelling, it is possible to raise the central density without affecting the edge and thus the limit can be exceeded without disruption, showing the transport deterioration itself.

We would not want to claim that deterioration of particle confinement is the only mechanism for density limit disruptions. We have already seen that the balance between radiation and input power can determine how much of the $n \sim I_p$ curve is accessible. For sufficiently dirty plasmas, radiation alone can cause the operating range to contract from all the operational boundaries [3, 27]. We have previously distinguished between two density limits on the basis of their scaling; perhaps it would be better to make the distinction on the basis of mechanism. The Murakami limit would apply to the operational limit, whatever its exact scaling on B_T, I_p and size, where radiation is the principal cause, and the

TABLE I. SUMMARY OF CALCULATIONS

I_p (kA)	$n_{peak}/\kappa\bar{J}$	n_{limit} (cm^{-3})	τ_n (ms)
370	1.2	4.3×10^{14}	51
220	2.0	2.6×10^{14}	19
220	2.4	2.1×10^{14}	7

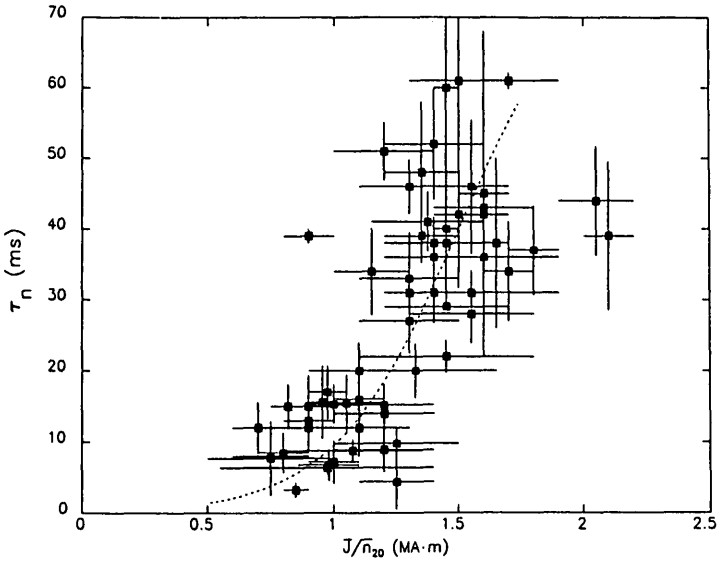

FIG. 12. Density decay time (after pellet injection) versus $\bar{J}/\bar{n}$. For Alcator, with $\kappa = 1$, the density limit is found at $\bar{J}/\bar{n} = 1$.

Hugill limit would apply to the operational limit where deterioration of particle confinement is the main cause. The mechanism that we propose allows us to connect the Hugill limit with the fuelling limit as well. Since the plasma density results from the balance of source and loss, deterioration of particle confinement with n/J can act in tandem with processes which reduce the particle source. This may also explain the observation that fuelling limits often show the $n_e \sim I_p$ scaling.

The same mechanism that we propose to explain the Hugill density limit may underlie the appearance of Marfes [28]. Marfes are bands of very high density, low temperature, poloidally asymmetric plasma that appear at the periphery of tokamak plasmas as the density limit is approached. Typically, Marfes occur at 60–80% of the density limit. They are believed to be a thermal condensation phenomenon [19, 29] localized by neoclassical flows in the edge plasma. If our new understanding of the density limit is correct, Marfes can be thought of as the first symptom of the deteriorating particle confinement. As particle confinement decreases, with energy confinement fixed, the ratio of power flux to particle flux at the edge also decreases. This means that there will be more particles at the edge and they will have lower average energy. These are just the right starting conditions for a thermal condensation. Of course, the details of the edge profiles, impurity content and plasma flows will affect the onset and characteristics of the Marfe.

4. SUMMARY

We have distinguished between several different density limits. The first – the Murakami limit – is caused by an unfavourable balance between input and radiated power and scales as $n \sim B_T/R$ for ohmically heated plasmas. The same physics could lead to a dependence on plasma current at lower densities. This limit is strongly affected by plasma purity and of course by auxiliary or alpha heating. With sufficient input power, the Murakami limit can be pushed to very high

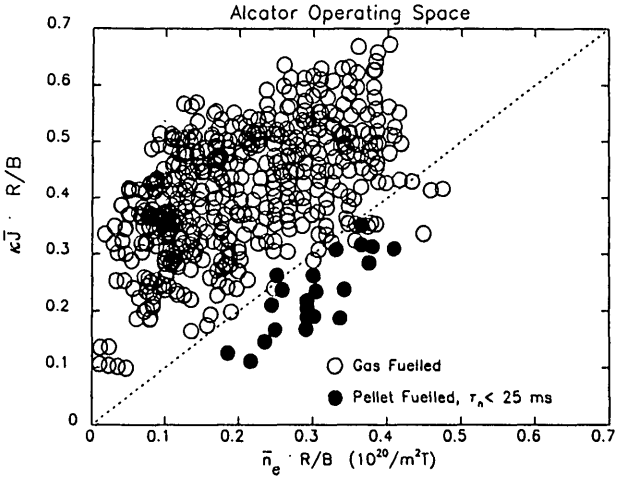

FIG. 13. DITE plot for Alcator C. The solid points are for pellet fuelled discharges with a fast decay of density.

values. The second density limit – the Hugill limit – depends principally on current density and plasma cross-section and may be due to a degradation in particle confinement time as the density limit is approached. Scaling this limit as $\bar{n} = \kappa \bar{J}$ brings much of the available database into line. In a sense, it is the most important density limit, since, together with the disruptive limit on plasma current ($q\psi > 2$), it defines the operating space for a tokamak and will yield the highest steady state density achievable on a given machine. For large and/or high density tokamaks or in the presence of processes which compete with the plasma for fuel, this limit may be difficult to reach. With particle confinement declining with n/J, any decrease in particle source will result in lower densities. Inadequate fuelling represents a third limit on density. All of the above limits must be obeyed; the operating space of a tokamak will be limited by the minimum of the Murakami, Hugill and fuelling limits.

ACKNOWLEDGEMENTS

The authors wish to thank the Alcator C, Doublet, ISX and PDX/PBX experimental groups for contributing data for this study. They also thank J. Sheffield and R. Stambaugh and other members of the Ignition Physics Study Group (IPSG) for the initial impetus and for many useful discussions.

REFERENCES

[1] MURAKAMI, M., CALLEN, J.D., BERRY, L.A., Nucl. Fusion **16** (1976) 347.
[2] PAUL, J.W.M., AXON, K.B., BURT, J., et al., in Plasma Physics and Controlled Nuclear Fusion Research 1976 (Proc. 6th Int. Conf. Berchtesgaden, 1976), Vol. 2, IAEA, Vienna (1977) 269.
[3] AXON, K.B., BAXTER, G.A., BURT, J., et al., in Plasma Physics and Controlled Nuclear Fusion Research 1978 (Proc. 7th Int. Conf. Innsbruck, 1978), Vol. 1, IAEA, Vienna (1979) 51.
[4] STOTT, P.E., HUGILL, J., FIELDING, S.J., et al., in Controlled Fusion and Plasma Physics (Proc. 8th Eur. Conf. Prague, 1979), Vol. 1, European Physical Society (1979) 151.
[5] GRANETZ, R., Phys. Rev. Lett. **49** (1982) 658.
[6] FIELDING, S.J., HUGILL, J., McCRACKEN, G.M., et al., Nucl. Fusion **17** (1977) 1382.
[7] BERRY, L.A., BUSH, C.E., CALLEN, J.D., et al., in Plasma Physics and Controlled Nuclear Fusion Research 1976 (Proc. 6th Int. Conf. Berchtesgaden, 1976), Vol. 1, IAEA, Vienna (1977) 49.
[8] VERSHKOV, V.A., MIRNOV, S.V., Nucl. Fusion **14** (1974) 383.
[9] AXON, K.B., CLARK, W.H.M., CORDEY, J.G., et al., in Plasma Physics and Controlled Nuclear Fusion Research 1980 (Proc. 8th Int. Conf. Brussels, 1980), Vol. 1, IAEA, Vienna (1981) 413.
[10] HUGILL, J., in Heating in Toroidal Plasmas (Proc. 2nd Joint Grenoble-Varenna Int. Symp. Como, 1980), CEC, Brussels (1980) 775.
[11] HUGILL, J., LOMAS, P.J., WOOTTON, A.J., et al., High Density Operation in DITE with Neutral Beam Injection, Rep. CLM-R239, UKAEA, Culham Laboratory, Abingdon, Oxfordshire (1983).
[12] SCHMIDT, G.L., MILORA, S.L., ARUNASALAM, V., et al., in Plasma Physics and Controlled Nuclear Fusion Research 1986 (Proc. 11th Int. Conf. Kyoto, 1986), Vol. 1, IAEA, Vienna (1987) 171.
[13] JET GROUP, Plasma Phys. Controll. Fusion **29** 10A (1987) 1219.
[14] WILSON, K.L., HSU, W.L., J. Nucl. Mater. **145-147** (1987) 121.
[15] DYLLA, H.F., LaMARCHE, P.H., ULRICKSON, M., et al., Nucl. Fusion **27** (1987) 1221.
[16] BELL, M., ARUNASALAM, V., BITTER, M., et al., Plasma Phys. Controll. Fusion **28** 9A (1986) 1329.
[17] FIORE, C., Massachusetts Institute of Technology, Cambridge, personal communication, 1986.
[18] MARMAR, E.S., RICE, J.E., TERRY, J.L., SEQUIN, F.H., Nucl. Fusion **22** (1982) 1567.
[19] GIBSON, A., Nucl. Fusion **16** (1976) 546.
[20] OHYABU, N., Nucl. Fusion **19** (1979) 1491.
[21] ASHBY, D.E.T.F., HUGHES, M.H., Nucl. Fusion **21** (1981) 911.
[22] WESSON, J., GOWERS, C., HAN, W., et al., in Controlled Fusion and Plasma Physics (Proc. 12th Eur. Conf. Budapest, 1985), Vol. 9F, Part I, European Physical Society (1985) 147.
[23] ROBERTS, D.E., Nucl. Fusion **23** (1983) 311.
[24] PERKINS, F.W., HULSE, R.A., Phys. Fluids **28** (1985) 1837.
[25] GREENWALD, M., BESEN, M., CAMACHO, F., et al., in Plasma Physics and Controlled Nuclear Fusion Research 1986 (Proc. 11th Int. Conf. Kyoto, 1986), Vol. 1, IAEA, Vienna (1987) 139.
[26] ALLEN, J., AUSTIN, G.E., AXON, K.B., et al., ibid., p. 227.
[27] PFEIFFER, W., WALTZ, R.E., Nucl. Fusion **19** (1979) 51.
[28] LIPSCHULTZ, B., LaBOMBARD, B., MARMAR, E.S., et al., Nucl. Fusion **24** (1984) 977.
[29] DRAKE, J., Phys. Fluids **30** (1987) 8.

(Manuscript received 29 March 1988
Final manuscript received 12 August 1988)